Macromolecular Chemistry and Physics
www.mcp-journal.de

# Role of Organic Phosphates and Phosphonates in Catalyzing Dynamic Exchange Reactions in Thiol-Click Vitrimers

*Khadijeh Moazzen, Elisabeth Rossegger, Walter Alabiso, Usman Shaukat, and Sandra Schlögl**

**Owing to their strong Brønsted acidity, organic phosphates and phosphonates are able to catalyze dynamic transesterification reactions in hydroxyl ester networks. Compared to commonly used transesterification catalysts, they are highly soluble in a wide range of acrylate monomers and neither affect cure kinetics nor shelf-life of photocurable acrylate and thiol-acrylate resins. Additionally, they promote fast stress relaxation and, by using derivatives with functional groups, are covalently incorporated within the photopolymer network. These salient features make organic phosphates and phosphonates ideal catalysts for the design and processing of photoreactive vitrimers. Herein, the catalytic activity of selected methacrylate-functional phosphates and vinyl-functional phosphonates on dynamic transesterifications are studied comprehensively. They are incorporated in a thiol-acrylate photopolymer providing functional –OH and ester moieties. Cure kinetics and thermomechanical properties are not significantly affected by the structure and functionality of the catalyst. In contrast, time-dependent stress relaxation measurements show that relaxation time and activation energy correlate well with the logarithmic acid dissociation constants of the Brønsted acids. The better understanding of the role of organic phosphates and phosphonates expands the scope of transesterification catalysts and is particularly interesting for the design of photoreactive vitrimers, which can be additively manufactured by using vat polymerization techniques.**

## 1. Introduction

Dynamic covalent bonds impart unique features such as self-healability, recyclability, malleability, and shape memory into polymer networks.[1] While the concept of dynamic covalent bonds can be realized by numerous reversible reaction pathways, the most intensively studied and widely applied one relies on the thermoactivated transesterification of hydroxyl ester moieties.[2] In particular, the pioneering work of Leibler et al. on malleable epoxy-based networks has become the starting point for exploiting transesterifications in the design of functional polymers.[3] Dynamic networks based on thermoactivated transesterifications are associative in nature and maintain their network connectivity at elevated temperature.[4] The thermally induced bond breakage and reformation reactions occur simultaneously and influence the viscoelastic properties of the dynamic networks at elevated temperature. Below the so-called topology freezing transition temperature ($T_v$), the exchange reactions are slow and the network properties are comparable to a classic thermoset. Above $T_v$, the exchange reactions are accelerated and the related topological rearrangements induce a viscoelastic flow of the network, which follows an Arrhenius trend.[3] Since vitreous silica shows a similar behavior, this new class of dynamic polymer networks was termed vitrimers. To enhance the exchange rate of thermoactivated transesterifications, catalysts are typically employed.[5,6] The selection of the catalyst is guided by parameters such as the catalyst's (in)solubility, temperature stability, and activity as well as long-term performance such as catalyst ageing or leaching.[7] Further considerations include undesirable catalyst migration, which has been addressed either by covalent attachment of the catalyst to the network[8] or the usage of polymeric catalysts.[9]

The most frequently used transesterification catalysts for vitrimers are organic zinc salts such as zinc acetate and zinc acetylacetonate, which activate the ester group by increasing its electrophilicity via polarization. In the presence of these Lewis acids, the reactive species are brought together through coordination bonds and the alcohol/alkoxide equilibrium is shifted toward higher nucleophilic alkoxide.[10] Apart from the classical epoxy-acid vitrimer of Leibler et al.,[5] organic zinc salts have been applied in numerous vitrimer systems such as composites from epoxidized natural rubber (ENR) cross-linked with either carboxyl group-functionalised carbon nanodots[11] or cellulose nanocrystals.[12] Other groups introduced $Zn(OAc)_2$ in silica-epoxy composites from diglycidyl ether of bisphenol A (DGEBA) and fatty acids[13] or in ENR-dodecanedioic acid

K. Moazzen, E. Rossegger, W. Alabiso, U. Shaukat, Dr. S. Schlögl
Polymer Competence Center Leoben GmbH
Roseggerstrasse 12, Leoben 8700, Austria
E-mail: sandra.schloegl@pccl.at

The ORCID identification number(s) for the author(s) of this article can be found under https://doi.org/10.1002/macp.202100072.

**DOI: 10.1002/macp.202100072**

 

networks.[14] Advancing from thermally cured networks, Zhang and co-workers used $Zn(OAc)_2$ to catalyze transesterifications in photocurable acrylate systems.[15] They reported that the dynamic acrylate photopolymers were able to rapidly relax stresses at 180 °C, and subsequently, demonstrated a thermo-activated healing and reshaping of 3D printed structures. However, the network design is limited as $Zn(OAc)_2$ is insoluble in commonly used acrylate monomers.

Other prominent types of transesterification catalysts are organic bases such as the guanidine base 1,5,7-triazabicyclo[4.4.0]dec-5-ene (TBD), whose catalytic activity relies on an enhancement of the nucleophilicity of the –OH moieties by H-bonding. TBD was shown to be an effective transesterification catalyst in composites from DGEBA and adipic acid filled with carbon nanotubes[16] or in epoxy-based composites containing graphene.[17] Recently, we have demonstrated that TBD also catalyzes transesterification reactions in hydrogenated and carboxylated nitrile butadiene rubber cross-linked with either bi-functional epoxides or epoxy-functionalized inorganic filler.[18] Although Bowman and co-workers successfully applied TBD for the preparation of dynamic thiol-ene networks, the catalyst suffers from several drawbacks when it comes to the processing and 3D printing of photocurable vitrimers.[19] On the one hand, it acts as radical scavenger and retards radically induced photopolymerization reactions. On the other hand, it catalyzes the thiol-Michael reaction in thiol-click resins, which leads to an immediate gelation of the resins.[20]

Along with the basic-catalyzed mechanism, the transesterification in vitrimers is also accelerated in the presence of Brønsted acids. In acid-catalyzed transesterifications, the electrophilicity of the carbonyl ester group is increased by protonation, which makes the carbonyl group more susceptible to a nucleophilic attack. A tetrahedral intermediate is formed by reaction with an –OH group in the network yielding a new ester bond by subsequent proton transfer, departure of the leaving group, and deprotonation.[21] Bates et al. studied the Brønsted acid-catalyzed transesterification in hydroxyl-functional polyesters and applied strong protic acids with a logarithmic acid dissociation constant (p*K*a) varying between –12 (triflic acid) and 0.81 (trichloroacetic acid).[22] They observed a distinctive stress relaxation, which increased with decreasing p*K*a value of the acid catalyst.

Recently, we have demonstrated the acid-catalyzed transesterification in thiol-acrylate photopolymers by using phosphate monoesters as strong Brønsted acids.[20] While mineral phosphates have been widely applied in the heterogeneous catalysis of transesterifications in solution,[23] we could show the catalytic activity of organic counterparts in solid polymer networks. Organic phosphates are ideal catalyst for developing photocurable vitrimers as they are not compromising on shelf-life or cure kinetics of photocurable acrylate and thiol-ene systems. In addition, due to their high solubility in a wide range of acrylate monomers they enable a facile tailoring of mechanical and thermal properties of vitrimers.

## 2. Results and Discussion

To get a better understanding of the catalytic activity of organic phosphates and phosphonates in photocurable vitrimers, we studied the performance of selected derivatives with varying logarithmic acid dissociation constants (p*K*a) (**Figure 1**a). The p*K*a values were taken from the literature and were referenced in $H_2O$. It should be noted that they are dependent on the medium/solvent in which they are measured, as they describe the thermodynamic equilibrium between a selected Brønsted acid and its conjugate base plus a proton.[24] When it comes to solid polyester vitrimers, Bates and co-workers proposed that the absolute p*K*a values might change but the relative trend should still hold.[22]

For this study, we selected ethylene glycol methacrylate phosphate (EGMP) and bis (2-methacryloyloxy)ethyl phosphate (DMEP), which are typically applied as corrosion inhibitors in polymeric coatings.[25] DMEP has a p*K*a value of 1.7,[26] while the p*K*a of EGMP amounts to 2.15.[27] Moreover, EGMP and DMEP bear methacrylate functions, through which they can be covalently incorporated into a photopolymer network.

Along with phosphates, we employed weaker organic phosphonates including vinyl phosphonic acid (VPA) and diethyl vinyl phosphonate (DEVP), which are popular precursors for functional polymers used in fuel cells or polyelectrolytic membranes.[28] Moreover, they comprise a terminal vinyl group for covalent attachment to the photopolymer network. While VPA has a p*K*a value of 2.74[29] DEVP does not contain any free –OH groups, and it is a very weak acid. For DEVP, there were no p*K*a data available in the literature, but we assume it is well above 20, as diethyl phenyl phosphonate has a p*K*a of 27.6.[30]

The catalysts were added to a photocurable thiol-acrylate formulation containing 50 mol% 2-hydroxy-3-phenoxy propyl acrylate, 25 mol% glycerol 1,3-diglycerolate diacrylate, 25 mol% trimethylolpropane tri(3-mercaptopropionate), and 2 wt% phenylbis(2,4,6-trimethylbenzoyl)phosphine oxide as photoinitiator (Figure 1b). Light triggered curing of the formulation yielded a thiol-acrylate photopolymer with ample –OH and ester groups, which are able to undergo dynamic exchange reactions in the presence of an appropriate transesterification catalyst (Figure 1c). For a direct comparison of the catalytic activity, the catalyst content was kept constant at 3.75 mol (related to the free –OH groups in the network). As the kinetics of dynamic exchange reactions is also governed by the network's chain mobility and cross-link density, we determined cure kinetics, cross-link density, and thermomechanical properties of the thiol-acrylate network as a function of the applied catalyst.[7,31]

In the first step, the photo-induced cure kinetics of the catalyzed formulations was monitored by FTIR spectroscopy and compared with a noncatalyzed one. FTIR spectra of a DMEP catalyzed network are provided as an example in Figure S1 (Supporting Information). **Figure 2**a provides the time-dependent depletion of the characteristic absorption bands of acrylate (1635 $cm^{-1}$) and thiol groups (2570 $cm^{-1}$). Both catalyzed and noncatalyzed thiol-acrylate formulations show a comparable cure rate and final conversion of the monomers is obtained upon 2 min UV exposure. The final acrylate conversion ranges between 80% and 83%, while the thiol conversion does not exceed 53%. The higher acrylate conversion is explained by the mixed-mode chain growth/step growth-like photopolymerization mechanism of the radical-mediated thiol-acrylate reaction. Due to their electron-withdrawing groups, acrylates exhibit a lower reactivity in thiol-ene reactions than electron-rich

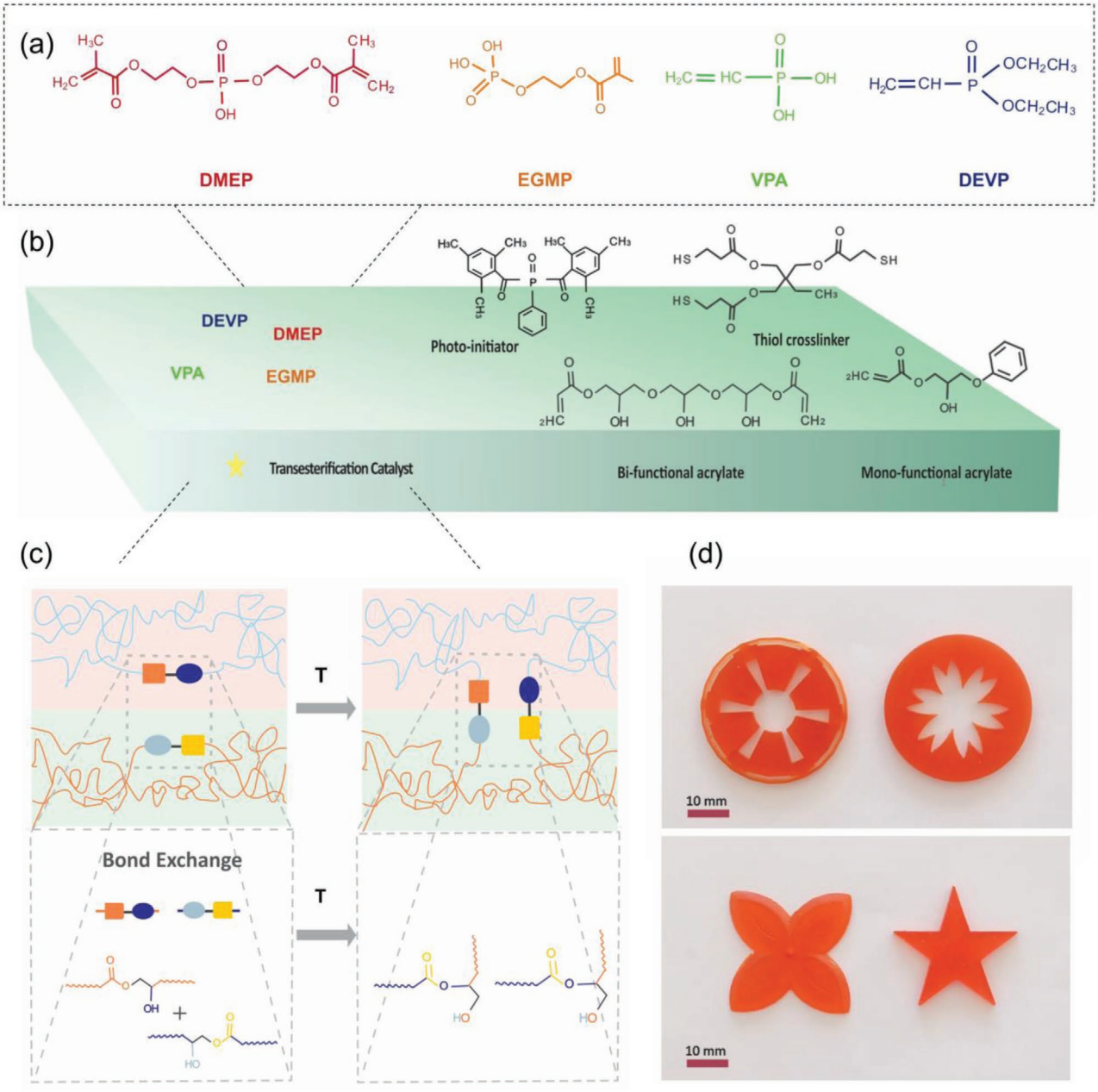


**Figure 1.** a) Organic phosphates and phosphonates used as transesterification catalysts in thiol-acrylate vitrimers. b) Photocurable monomers, cross-linker, and photoinitiator used for the preparation of the thiol-acrylate matrix. c) Schematic representation of dynamic exchange reactions in thiol-acrylate vitrimers relying on thermoactivated transesterifications. d) Digital light processing (DLP) 3D printed test structures comprising a height of 2 mm.

alkenes.[32] Consequently, the acrylate radicals are not only participating in chain transfer reactions but also in propagation reactions, yielding heterogeneous networks with intertwined thiol-ene and homopolymerized acrylate segments.[33]

The broad tan delta curves obtained from dynamic mechanical analysis (DMA) confirm the heterogeneous network structure of the investigated thiol-acrylate networks (Figure 2d). While the cure kinetics showed a comparable final monomer conversion of the networks under investigation, the DMA data reveal that the networks slightly differ in their network heterogeneity. The glass transition region ($T_g$) ranges from –15 °C to 45 °C, showing its maximum of tan delta between 3 °C and 8 °C. With a storage modulus of 0.8–1.5 MPa at 20 °C (Figure 2c), the networks are flexible but reasonably stiff to produce free-standing objects. Together with the fast cure speed and the high storage stability of the resins, these features enable a facile 3D printing of polymeric structures via digital light processing (DLP) (Figure 1d).

To determine the cross-linking density of the catalyzed and noncatalyzed thiol-acrylate systems, equilibrium swelling

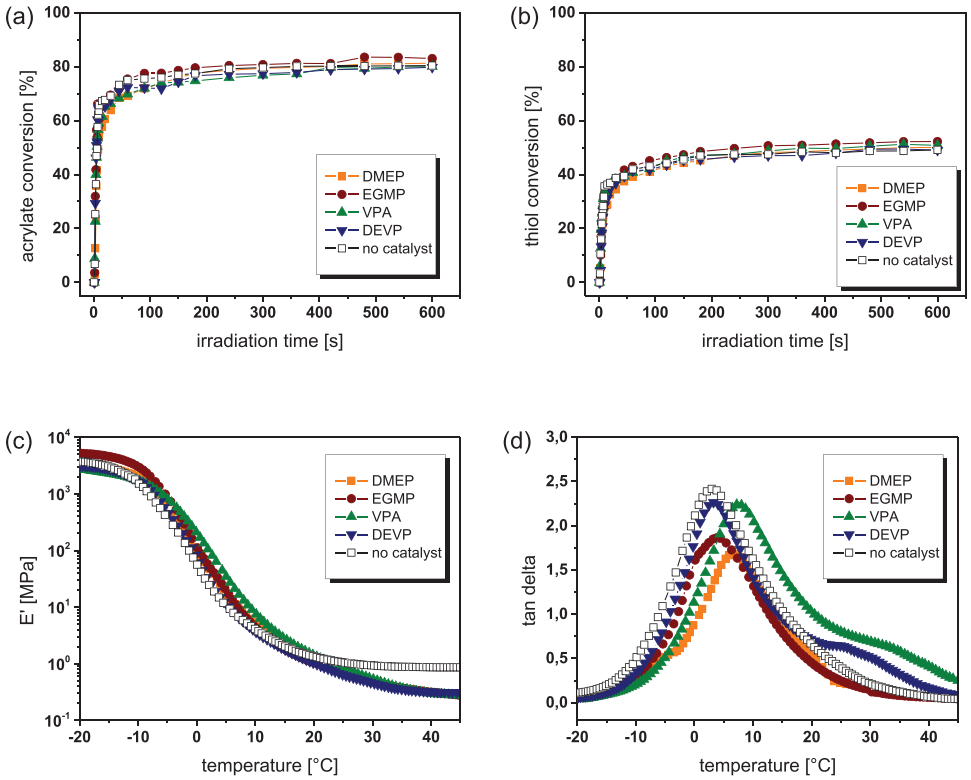


**Figure 2.** Following the cure kinetics in catalyzed and noncatalyzed thiol-acrylate formulations by FTIR spectroscopy. The normalized peak area of the IR absorption bands of the a) acrylate groups (1635 $cm^{-1}$) and b) thiol groups (2570 $cm^{-1}$) is plotted against exposure time. Irradiation ($\lambda$ = 420–450 nm, 3.3 mW $cm^{-2}$) was performed under air. The lines are a guide for the eye. c) Storage modulus and d) tan delta curves of cured thiol-acrylate formulations as a function of temperature, plotted for various transesterification catalysts.

measurements were conducted in dichloromethane. For sample preparation, discs with a diameter of 10 mm were DLP 3D printed (**Table 1**). The gel content varies between 63.5 ± 2.1 and 70.4 ± 1.4%, is slightly higher for catalyzed networks, and decreases with increasing acidity of the catalyst.

In general, the low gel content can be explained by residual acrylate monomers as well as thiol cross-linker, which have not been incorporated within the photopolymer during the curing reaction and are extracted from the swollen networks. However, the increasing gel content indicates a higher cross-link density of the related networks. This is also confirmed by the mass swelling ratios, which gradually decrease from noncatalyzed to DMEP catalyzed networks. The rising cross-linking density might be explained by acid-catalyzed thiol-ene reactions, which proceed during storage of the cured samples under dark conditions.[34] We observed acid-catalyzed dark reactions of the thiol-acrylate resin at higher catalyst contents. While at 3.75 mol%, the resin is stable over more than 1 week, a premature gelation occurs within 24 h if the catalyst content is exceeding 15 mol%. To confirm the occurrence of post-curing reactions, we studied the progress of the acrylate and thiol conversion of the DMEP catalyzed network under dark conditions. For this, the network was irradiated until reaching maximum final monomer conversion and then stored at room temperature for 24 h. The data clearly reveal a further increase of the acrylate (from 81% to 84%) and thiol conversion (from 53% to 56%) upon prolonged storage at room temperature. From the results it can be concluded that the employed organic phosphates and phosphonates do not compromise on the photocure kinetics but induce acid-catalyzed dark reactions, which increase the cross-link density of the catalyzed thiol-acrylate networks.

**Table 1.** Properties of catalyzed and noncatalyzed thiol-acrylate networks.

| Catalyst | *E'* at 20 °C [MPa] | $T_g$ [°C] | $T_v$ [°C] | Mass swelling ratio | Gel content [%] |
|---|---|---|---|---|---|
| Without | 1.03 | 3 | – | 17.8 ± 1.5 | 63.5 ± 2.1 |
| DEVP | 0.98 | 3 | 49 | 16.5 ± 0.3 | 64.6 ± 1.3 |
| VPA | 1.32 | 8 | 50 | 14.5 ± 0.4 | 66.2 ± 1.3 |
| EGMP | 1.30 | 4 | 55 | 13.1 ± 0.6 | 67.4 ± 2.2 |
| DMEP | 1.25 | 7 | 59 | 12.7 ± 1.6 | 70.4 ± 1.4 |

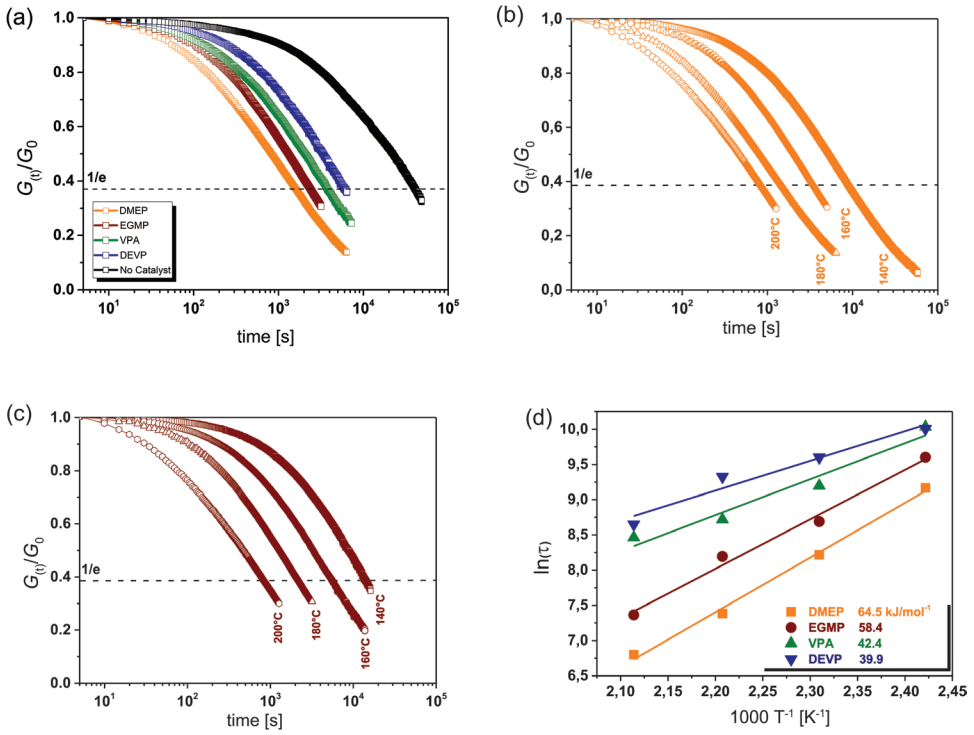


**Figure 3.** a) Normalized stress relaxation curves of catalyzed and noncatalyzed thiol-acrylate networks obtained at 180 °C. Normalized stress relaxation curves of b) DMEP and c) EGMP catalyzed thiol-acrylate networks obtained at 140 °C, 160 °C, 180 °C, and 200 °C. d) Arrhenius plots of catalyzed thiol-acrylate networks derived from the measured relaxation times.

The catalytic activity of the compounds was compared in subsequent temperature-dependent stress relaxation studies. For sample preparation, discs with a diameter of 10 mm were printed with DLP 3D printing. The stress relaxation of the networks was measured between 140 °C and 200 °C. Under the applied conditions, the chain segments of the low-*Tg* networks are highly mobile and facilitate bond exchange reactions. **Figure 3**a shows the time-dependent evolution of the relaxation modulus at 180 °C for noncatalyzed as well as catalyzed thiol-acrylate systems (Figure 3a). As reported in previous work, the thiol-acrylate network exhibits a slight stress relaxation, even in the absence of a transesterification catalyst.[20] This is attributed to a thermal release of volumetric shrinkage stresses arising during network evolution.[35]

In the presence of the protic Brønsted acids DMEP, EGMP, and VPA, a fast relaxation is observed, whose reaction rate increases with decreasing p*Ka* value. Even at a higher cross-linking degree, the DMEP catalyzed network only requires 15 min to relax 63% of the initial stress. In contrast, the lower cross-linked VPA catalyzed network needs 62 min under the same conditions. From the results it is concluded that the exchange rate is mainly governed by the acidity of the catalyst, while the cross-link density (at least in the investigated range of the networks) plays a minor role.

Interestingly, the nonprotic and nearly neutral dialkyl alkylphosphonate DEVP is also able to accelerate transesterifications in thiol-acrylate photopolymers, albeit at a lower rate than the protic catalysts. We assume that the compound contains not fully esterified by-products, whose –OH groups might be able to efficiently catalyze transesterifications. This is also confirmed by the FTIR spectrum of neat DEVP revealing a distinctive band related to –OH groups between 3693 and 3315 cm$^{-1}$ (Figure S2, Supporting Information). The presence of acidic –OH groups would also explain the ability of the resin to undergo acid-catalyzed dark reactions as the cross-link density is slightly higher than the reference system containing no catalyst (Table 1).

The stress relaxation of the four catalyzed networks is clearly temperature-dependent (Figure 3b,c and Figure S3a,b, Supporting Information) and characteristic for dynamic networks, in which the bond exchange rate increases with rising temperature.[2]

In vitrimers, the relaxation time ($\tau^*$) follows an Arrhenius-type temperature dependency $\tau^* = \tau_0 \exp(E_a/RT)$, in which $E_a$ corresponds to the activation energy and $R$ is the universal gas constant.[6,18] According to the Maxwell Model, $\tau^*$ can be derived from the measured relaxation data by taking the normalized relaxation modulus ($G_{(t)}/G_0$) required to relax e$^{-1}$ (37%) of the initial stress.[6] In Figure 3c, $\tau^*$ is plotted against ($1/T$) in a semilogarithmic scale and the linear trend obtained for all four catalyzed systems confirms the Arrhenius-type temperature dependence and the vitrimeric nature of the network.[7,30]

The activation energy ($E_a$) of the catalyzed networks was determined, by taking the slope ($m = E_a/R$) of the straight line fitted to the data. The results reveal that vitrimers catalyzed with stronger Brønsted acids have higher $E_a$ values, which indicates a higher temperature-dependency of the networks' exchange kinetics. The same trend was also found by Bates et al. in low-*Tg* polyester networks at temperatures between 25 °C

and 60 °C.[22] By using strong Brønsted acids with p*K*a values ranging from −12 to 0.81, they were able to obtain $E_a$ values between 49.6 and 66.7 kJ mol$^{-1}$. It is interesting to note that in the thiol-acrylate vitrimers under investigation, the relaxation times and their temperature dependence can be adjusted over a similar range (42.4–64.5 kJ mol$^{-1}$), with protic catalysts spanning a narrower range of p*K*a values (1.29–2.11). For DEVP, the lowest *E*a value is obtained (39.9 kJ mol$^{-1}$), which is explained by the low acidity of the dialkyl alkylphosphonate.

From the results it can be concluded that the exchange reactions in thiol-acrylate vitrimers are very sensitive to the acidity of the phosphate or phosphonate catalyst with stronger Brønsted acids giving rise to higher $E_a$ values and faster relaxation rates. The difference in the exchange kinetics also directly affects the $T_v$, at which the network changes from a viscoelastic solid to a viscoelastic liquid.[7] The $T_v$ values were derived by extrapolation of the fitted data to a relaxation time of $10^6$ s and are given in Table 1. The $T_v$ data correlate well with the p*K*a value of the catalysts and the $E_a$ values of the related dynamic networks and gradually increases from 49 °C to 59 °C. The results clearly show that organic phosphates and phosphonates are versatile catalysts in accelerating dynamic exchange reactions in vitrimeric photopolymers and based on their acidity enable a convenient tuning of exchange kinetics and $T_v$. In addition, Brønsted acids exhibit a better performance in catalyzing transesterifications in vitrimers compared to Lewis acid catalysts such as $Zn(OAc)_2$.[22] While lower cross-linked acrylate networks with $Zn(OAc)_2$ require 120 min (at 180 °C) to relax 63% of the initial stress, the DMEP catalyzed thiol-acrylate is nearly ten times faster (15 min) under the same conditions.[15] Even in the DEVPcatalyzed network the initial stress is being relaxed within shorter time (102 min) giving rise to the superior activity of organic phosphates and phosphonates in thiol-click vitrimers relying on transesterifications.

## 3. Conclusion

In this study, organic phosphates and phosphonates were exploited to catalyze reversible transesterifications in photocurable thiol-click vitrimers. The low-*T*g networks were highly mobile at elevated temperature and facilitated bond exchange reactions, whose rate was sensitive to the acidity of the applied catalyst. $E_a$ values and relaxation rate increased with increasing p*K*a value of the catalyst giving rise to a higher temperature-dependency of the networks' exchange kinetics. Along with exchange kinetics, the acidity of the catalyst directly affected the $T_v$, which increased from 49 to 59 °C. The study further revealed that protic organic phosphates are superior in catalyzing dynamic exchange reactions in vitrimeric photopolymers. In particular, DMEP catalyzed networks are up to 10 times faster to relax stresses at a given temperature compared to vitrimers containing typical Lewis acids.

## 4. Experimental Section

*Materials and Chemicals*: EGMP containing up to 25% of diester, was supplied by Gute Chemie, Germany. VPA, DEVP and Sudan II were purchased from Tokyo Chemical Industry Co., Japan. Trimethylolpropane tri(3-mercaptopropionate) was obtained from Bruno Bock Chemische Fabrik GmbH & Co. KG, Germany. All other chemicals, including bis (2-methacryloyloxy ethyl) phosphate (DMEP), 2-hydroxy-2-phenoxypropyl acrylate, glycerol 1,3-diclycerolate diacrylate, and phenylbis(2,4,6-trimethylbenzoyl) phosphine oxide were purchased from Sigma-Aldrich and used as received.

*Sample Preparation*: 2-hydroxy-3-phenoxy propyl acrylate (50 mol%) was added to glycerol 1,3-diclycerolate diacrylate (25 mol%) in a light-protected vessel along with one of the catalysts (3.75 mol% related to –OH groups) and mixed. An amount of 0.05 wt% Sudan II was added, and the formulation underwent ultrasonication until the dissolution of the photoabsorber. The mixtures were then supplemented with 2 wt% phenylbis(2,4,6-trimethylbenzoyl) phosphine oxide and 25 mol% trimethylolpropane tri(3-mercaptopropionate) and were stirred at 100 rpm at room temperature. Accordingly, four formulations were prepared, and for each formulation, one of the catalysts (ethylene glycol methacrylate phosphate, bis (2-methacryloyloxy ethyl phosphate), vinyl phosphonic acid, or diethyl vinyl phosphonate) was used. In addition, one formulation was prepared without a catalyst as a reference.

*Characterisation of Cure Kinetics and Network Properties*: A Vertex 70 FTIR spectrometer (Bruker, USA) was used to follow the curing process induced by light. Sixteen scans were collected in transmission mode between 4000 cm$^{-1}$ and 700 cm$^{-1}$ with a resolution of 4 cm$^{-1}$, and the measurement of the absorption peak area was facilitated using OPUS software. An amount of 1.5 µL of each resin formulation was drop cast between two $CaF_2$ discs, and curing was carried out by a light-emitting diode lamp (zgood wireless LED curing lamp), which led to a power density of 3.3 mW cm$^{-2}$ ($\lambda$ = 420–450 nm). The curing process was followed up to 600 s light exposure until the characteristic carbonyl and thiol peaks ceased to change in intensity. The conversion rates were calculated from the normalized intensity of C=C and S–H peaks using OPUS software.

Stress relaxation analysis was carried out in a moving die rheometer (Anton Paar, Austria) at 140 °C, 160 °C, 180 °C, and 200 °C. Prior to measurement, the specimens were equilibrated at 20 N at the selected analysis temperature for 20 min. Then, a 3% step strain was applied, and the stress was recorded over-time until 37% relaxation was achieved.

DMA was carried out by exploiting a dynamic mechanical analyzer (DMA/SDTA861e, Mettler-Toledo GmbH, Switzerland) on samples with the width of 4.5 mm, and a thickness of 1 mm with a clamping distance of 10.5 mm in tensile mode. The scans were performed between −20 and 90 °C using a heating rate of 2 °C min$^{-1}$ with a frequency of 1 Hz, and maximum amplitude of 10 µm.

For equilibrium swelling measurements, discs with a diameter of 10 mm were 3D DLP printed and immersed in dichloromethane at 23 °C for 48 h. After the excess solvent on the surface was removed carefully using tissue paper, the weight of the swollen gel was determined. The samples were then dried at 40 °C until constant weight and reweighed to obtain the gel contents. Mass swelling ratios were determined by $(m_s - m_d)/m_d$ with $m_s$ being the mass of the swollen sample and $m_d$ its initial mass. Five samples were tested for each network and the arithmetic average was taken.

*Bottom-Up Digital Light Processing 3D Printing*: Three-dimensional (3D) DLP printing was carried out using an Anycubic Photon Zero printer (China) supplied with a LED 405 nm light source. Two bottom layers were exposed for 20 s, while the other layers were irradiated for 8 s. The circular specimens were set to be prepared with a height of 50 µm using a building speed of 3 mm s$^{-1}$, and a retracting speed of 3 mm s$^{-1}$. To carry out the post-curing process, specimens were heated at 60 °C for 20 min in an oven. Then, the curing was completed by subsequent UV irradiation using microwave-powered UV-lamp with dichroic reflector, constant UV-emission, bulb length of 250 mm, and a power of 249 W cm$^{-1}$.

## Supporting Information

Supporting Information is available from the Wiley Online Library or from the author.

## Acknowledgements

Part of the research work was performed with the "SMART" project. This project has received funding from the European Union's Horizon 2020 research and innovation programme under the Marie Sklodowska-Curie grant agreement No 860108.

Part of the research work was performed also within the COMET-Module "Chemitecture" (project-no.: 21 647 048) at the Polymer Competence Center Leoben GmbH (PCCL, Austria) within the framework of the COMET-program of the Federal Ministry for Transport, Innovation and Technology and the Federal Ministry for Digital and Economic Affairs with contributions by the Institute of Chemistry of Polymeric Materials (Montanuniversitaet Leoben, Austria). The PCCL is funded by the Austrian Government and the State Governments of Styria, Upper and Lower Austria.

## Conflict of Interest

The authors declare no conflict of interest.

## Data Availability Statement

Research data are not shared.

## Keywords

catalyst, organic phosphates, organic phosphonates, thermoactivated transesterification, vitrimers

Received: February 26, 2021
Revised: March 22, 2021
Published online: April 14, 2021

[1] a) C. J. Kloxin, C. N. Bowman, *Chem. Soc. Rev.* **2013**, *42*, 7161; b) W. Alabiso, S. Schlögl, *Polymers* **2020**, *12*, 1660.
[2] J. M. Winne, L. Leibler, F. E. Du Prez, *Polym. Chem.* **2019**, *10*, 6091.
[3] D. Montarnal, M. Capelot, F. Tournilhac, L. Leibler, *Science* **2011**, *334*, 965.
[4] N. J. van Zee, R. Nicolaÿ, *Prog. Polym. Sci.* **2020**, *104*, 101233.
[5] D. Montarnal, M. Capelot, F. Tournilhac, L. Leibler, *Science* **2011**, *334*, 965.
[6] M. Capelot, M. M. Unterlass, F. Tournilhac, L. Leibler, *ACS Macro Lett.* **2012**, *1*, 789.
[7] W. Denissen, J. M. Winne, F. E. Du Prez, *Chem. Sci.* **2016**, *7*, 30.
[8] F. I. Altuna, C. E. Hoppe, R. J. J. Williams, *Eur. Polym. J.* **2019**, *113*, 297.
[9] X. Niu, F. Wang, X. Li, R. Zhang, Q. Wu, P. Sun, *Ind. Eng. Chem. Res.* **2019**, *58*, 5698.
[10] A. Demongeot, S. J. Mougnier, S. Okada, C. Soulié-Ziakovic, F. Tournilhac, *Polym. Chem.* **2016**, *7*, 4486.
[11] Z. Tang, Y. Liu, B. Guo, L. Zhang, *Macromolecules* **2017**, *50*, 7584.
[12] L. Cao, J. Fan, J. Huang, Y. Chen, *J. Mater. Chem. A* **2019**, *167*, 421.
[13] A. Legrand, C. Soulié-Ziakovic, *Macromolecules* **2016**, *49*, 5893.
[14] Z. Feng, J. Hu, H. Zuo, N. Ning, L. Zhang, B. Yu, M. Tian, *ACS Appl. Mater. Interfaces.* **2018**, *11*, 1469.
[15] B. Zhang, K. Kowsari, A. Serjouei, M. L. Dunn, Q. Ge, *Nat. Commun.* **2018**, *9*, 1831.
[16] Y. Yang, Z. Pei, X. Zhang, L. Tao, Y. Wei, Y. Ji, *Chem. Sci.* **2014**, *5*, 3486.
[17] Z. Yang, Q. Wang, T. Wang, *ACS Appl. Mater. Interfaces* **2016**, *8*, 21691.
[18] a) S. Kaiser, S. Wurzer, G. Pilz, W. Kern, S. Schlögl, *Soft Matter* **2019**, *15*, 6062; b) S. Kaiser, J. N. Jandl, P. Novak, S. Schlögl, *Soft Matter* **2020**, *16*, 8577.
[19] G. B. Lyon, L. M. Cox, J. T. Goodrich, A. D. Baranek, Y. Ding, C. N. Bowman, *Macromolecules* **2016**, *49*, 8905.
[20] E. Rossegger, R. Höller, D. Reisinger, J. Strasser, M. Fleisch, T. Griesser, S. Schlögl, *Polym. Chem.* **2021**, *117*, 10212.
[21] a) E. Lotero, Y. Liu, D. E. Lopez, K. Suwannakarn, D. A. Bruce, J. G. Goodwin, *Ind. Eng. Chem. Res.* **2005**, *44*, 5353; b) P. A. Alaba, Y. M. Sani, W. M. Ashri Wan Daud, *RSC Adv.* **2016**, *6*, 78351.
[22] J. L. Self, N. D. Dolinski, M. S. Zayas, J. Read de Alaniz, C. M. Bates, *ACS Macro Lett.* **2018**, *7*, 817.
[23] a) F. Bazi, H. El Badaoui, S. Sokori, S. Tamani, M. Hamza, S. Boulaajaj, S. Sebti, *Synth. Commun.* **2006**, *36*, 1585; b) K. Thinnakorn, J. Tscheikuna, *Appl. Catal., A* **2014**, *476*, 26.
[24] E. M. Arnett, G. W. Mach, *J. Am. Chem. Soc.* **1966**, *88*, 1177.
[25] A. Farahi, F. Bentiss, C. Jama, M. A. El Mhammedi, M. Bakasse, *J. Alloys Compd.* **2017**, *723*, 1032.
[26] U. Salz, A. Mucke, J. Zimmermann, F. R. Tay, D. H. Pashley, *J. Adhes. Dent.* **2006**, *8*, 143.
[27] B. Danko, A. W. Trochimczuk, Z. Samczyński, A. Hamerska-Dudra, R. S. Dybczyński, *React. Funct. Polym.* **2007**, *67*, 1651.
[28] L. Macarie, G. Ilia, *Prog. Polym. Sci.* **2010**, *35*, 1078.
[29] B. Bingöl, W. H. Meyer, M. Wagner, G. Wegner, *Macromol. Rapid Commun.* **2006**, *27*, 1719.
[30] D. H. Ripin, D. A. Evans, *pKa's of Inorganic and Oxoacids*, Chem *206*, **2005**.
[31] L. Imbernon, S. Norvez, L. Leibler, *Macromolecules* **2016**, *49*, 2172.
[32] C. E. Hoyle, T. Y. Lee, T. Roper, *J. Polym. Sci., Part A: Polym. Chem.* **2004**, *42*, 5301.
[33] a) A. F. Senyurt, H. Wei, C. E. Hoyle, S. G. Piland, T. E. Gould, *Macromolecules* **2007**, *40*, 4901; b) T. Y. Lee, T. M. Roper, E. S. Jonsson, C. A. Guymon, C. E. Hoyle, *Macromolecules* **2004**, *37*, 3606; c) S. K. Reddy, K. S. Anseth, C. N. Bowman, *Polymer* **2005**, *46*, 4212; d) M. Sahin, S. Ayalur-Karunakaran, J. Manhart, M. Wolfahrt, W. Kern, S. Schlögl, *Adv. Eng. Mater.* **2017**, *19*, 1600620.
[34] B. P. Sutherland, M. Kabra, C. J. Kloxin, *Polym. Chem.* **2021**, *38*, 646.
[35] J. Chen, S. Jiang, Y. Gao, F. Sun, *J. Mater. Sci.* **2018**, *53*, 16169.